# Small-Scale Climate Maps: A Sensitivity Analysis of Some Common Assumptions Associated with Grid-Point Interpolation and Contouring

Cort J. Willmott, Clinton M. Rowe, *and* William D. Philpot

ABSTRACT. From Shepard's (1968) local-search method, algorithms are developed for contouring on spherical surfaces and in Cartesian two-space. These algorithms are used to investigate errors on small-scale climate maps caused by the common practice of interpolating—from irregularly-spaced data points to regular-lattice nodes—and contouring in Cartesian two-space. Using mean annual air temperatures drawn from 100 irregularly-spaced weather stations, the annual air-temperature field over the western half of the northern hemisphere is estimated both on the sphere (assumed to be correct) and in Cartesian two-space. When these fields are mapped and compared, error magnitudes as large as 5° to 10° C appear in the air-temperature field approximated in Cartesian two-space.

KEY WORDS: climate, surface mapping, interpolation, contouring

Within climatology, automated point interpolation and isoline construction have progressively supplanted draftsmen's relatively subjective methods. Cartographers have devised numerous digital algorithms for interpolation from irregularly-spaced data points in Cartesian two-space to the nodes of a regular lattice, and isoline placement among the estimated grid-point values (Peucker 1980; Rhind 1975; Morrison 1974; Marble 1981). It is uncommon in climatology, although possible, to draw isolines directly from the irregularly-spaced data, ostensibly because the grid-point values are frequently required for subsequent analyses.

A subset of atmospheric research, under the rubric "objective analysis," constitutes another source of potentially useful interpolation and contouring procedures (Panofsky 1949; Cressman 1959; Barnes 1964; Fritsch 1971; Gandin 1963; Schlatter, Branstator, and Thiel 1976; Wahba and Wendelberger 1980). In many ways, the development of objective analysis parallels the advancements in cartographic interpolation and contouring, except that the impetus for and direction of objective analytic research have largely been determined by the requirements of the weather-forecasting community. Objective analysis, as a result, characteristically relies upon the typically smooth nature of upper-air data, as well as upon multivariate and autocorrelative relationships beyond those contained in the irregularly-spaced scalar field associated with a single variable. Many objective functions, for these reasons, may be inappropriate for mapping the characteristically uneven scalar fields associated with near-surface climate, al-

C. Willmott is an Associate Professor in the Department of Geography and C. Rowe a doctoral student and Research Assistant at the Center for Climatic Research, University of Delaware, Newark DE 19716. W. Philpot is an Assistant Professor in the Remote-Sensing Program, School of Civil and Environmental Engineering, Cornell University, Ithaca, NY 14853. They thank James Burt, Franklin Gossette, David Legates, and Yale Mintz for insights and technical assistance, and the Laboratory for Atmospheric Sciences at NASA's Goddard Space-Flight Center for financial support (NASA grant NAG 5-107).


0094-1689/85$2.50

though the objective-analysis literature contains a number of innovative approaches to interpolation (Wahba 1979 and 1981; Wahba and Wendelberger 1980).

Most objective functions, like interpolation and contouring procedures developed by cartographers, tacitly assume that data values have been projected into Cartesian two-space (Wahba and Wendelberger 1980). Only occasionally have the true relationships between the data and grid points on the surface of the earth or sphere been preserved and explicitly incorporated into an objective algorithm (Wahba 1979 and 1981).

Point interpolation and isoline construction in climatology characteristically begin with the collection of data values associated with an irregularly distributed set of points on the surface of the earth. For most climatological purposes, the earth can be assumed perfectly spherical, with a trivial loss of accuracy, and each data observation (subscript $i$) of the variable of interest, $z_i(\lambda,\phi)$, can be uniquely located by simple longitude ($\lambda$) and latitude ($\phi$) coordinates. Once the data points have been compiled, they are usually projected into a Cartesian two-space so that each $z_i(\lambda,\phi)$ becomes $z_i(x,y)$, and one of the readily available Cartesian-based interpolation and contouring algorithms (Marble 1981) can be applied to the data. Many times the projection is indirectly accomplished by the estimation of $x$ and $y$ from an existing map or by the scaled, but otherwise unaltered, assignment of $\lambda$ and $\phi$ to $x$ and $y$, respectively. Estimates of $z_j(x,y)$ then are made at the nodes (subscript $j$) of a regular lattice by point interpolation, ordinarily followed by the lacing of isolines through the lattice of interpolated values. During contour lacing, the points—grid points in this case—are once again assumed to be correctly related by the projected Cartesian geometry. Assumed Cartesian relationships between the projected points, in other words, underlie the interpolation of grid-point values and often contribute twice to the estimation of isoline locations.

In the mapping of climate fields that extend over large areas of the earth's surface, however, spherical distance and directional relationships cannot be accurately preserved in translation to Cartesian two-space. Subsequent interpolation and contouring, based on the projected relationships, will necessarily be in error. The magnitude of the errors, of course, will depend completely on the map projection selected, the distribution of data and grid points, and the properties of the interpolation and contouring algorithm. These errors can be large.

To avoid the propagation of such error in small-scale mapping, climatologists should perform their interpolation and contouring on the surface of the sphere, namely, in "spherical space." That is, the interpolation and contouring processes should depend only upon the spherical geometry that relates the grid and data points on the earth's surface. Only after the grid-point values and contour positions have been determined on a sphere should they be projected onto a map.

Even though most climatological papers do not describe or even cite the interpolation and contouring methods from which their climate maps were generated, errors that derive from Cartesian-based interpolations are commonplace. Any of the numerous SYMAP (Shepard 1968), IMSL (Akima 1978), or SURFACE II (Sampson 1978) computed contour maps, for example, assume a Cartesian space. On any given small-scale climate map, particularly when the algorithm is not described, the nature and degree of error may be difficult to ascertain. In cases where the mapped area extends to one or both of the poles or over all 360 degrees of longitude, however, two symptoms stand out. Cylindrical projections having as their edges the north or south pole and the dateline, for instance, typically exhibit multiple isolines crossing the poles and contours which do not meet at the dateline (Schlatter, Branstator, and Thiel

1976; Halem, Kalney, Baker, and Atlas 1982; Rivin and Kulikov 1982). Climatologists have largely overlooked interpolation and contouring errors produced by the projection of data points into Cartesian space prior to grid-point interpolation and contouring.

To examine the degree to which Cartesian-based interpolation and contouring can distort the small-scale mapping and analysis of climate fields, we present the results of two sets of map analyses based upon two modified versions of Shepard's (1968) interpolation algorithm, augmented with two contour-lacing routines to permit the plotting of isolines. We selected Shepard's (1968) function as a benchmark procedure because of its widespread use (by 1980, in the form of SYMAP, it was implemented at well over 500 organizations) and because it represents a class of point-interpolation algorithms that have an intuitive appeal (Shepard 1968) and are "relatively robust" (Rhind 1975, p. 299).

Our first implementation of Shepard's method is quite similar to SYMAP's, inasmuch as all interpolations and isoline determinations assume that the data and grid points are correctly related in Cartesian two-space. Our second, "spherically based," version computes all interpolations and isoline positions from the actual data and grid-point locations on the surface of the sphere. Longitude and latitude coordinates associated with each spherically-derived isoline are then projected along with all other substantive elements of the map onto a Cartesian two-space.

Following descriptions of these two algorithms—with emphasis on spherically-based procedures—we describe results obtained from comparative mappings of an average annual air-temperature field sampled from a recently compiled world-climate data set (Willmott, Mather, and Rowe 1981). In other words, our two implementations of Shepard's function follow, succeeded by an examination of two air-temperature maps derived from combinations of the air-temperature field, two well-known cylindrical projections, and our two sets of interpolation and contouring algorithms.

## Grid-Point Interpolation

Shepard's interpolation function estimates a value at each node of a predetermined lattice from a small number of nearby data points. Developed for interpolation within Cartesian two-space, the procedure accounts for the distance and directional relationships between neighboring data and grid points (Figure 1). The algorithm also has a limited extrapolation capability that permits grid points to take on values outside the range of the data. Although there are a few important differences between the algorithms described here and Shepard's original function, the essence of his function remains.

Based upon a simple gravity hypothesis and other considerations (Shepard 1968 and 1984), the interpolation procedure requires that the value of each nearby data point influence the estimation of the associated grid-point value by an amount proportional to the intervening distance. Weights are ascribed to three categories of distance according to

$$S_k = \begin{cases} d_{j,k}^{-1}, & d_{j,k} \le r_j/3 \\ \dfrac{27}{4r_j}\left(\dfrac{d_{j,k}}{r_j} - 1\right)^2, & r_j/3 < d_{j,k} \le r_j \\ 0, & d_{j,k} > r_j, \end{cases} \quad (1)$$

where $r_j$ is the search radius and $d_{j,k}$ is the distance from grid point $j$ to nearby data point $k$. The subscript $k$ (and later $l$) is used to reference one of those data points near $j$ that belongs to the set of data points influencing the interpolated value at $j$. Following Shepard, the search radius is initially defined as a constant, that is, as the radius of a circle (on either a plane or a sphere) that contains an average of 7 data points. In cases where fewer than 4 or more than 10 data points fall within $r_j$ of $j$, $r_j$ is adjusted. When the former occurs, $r_j$ is set equal to the distance of the fifth-closest data point, whereas in the latter case, $r_j$ is redefined as the distance to the elev-

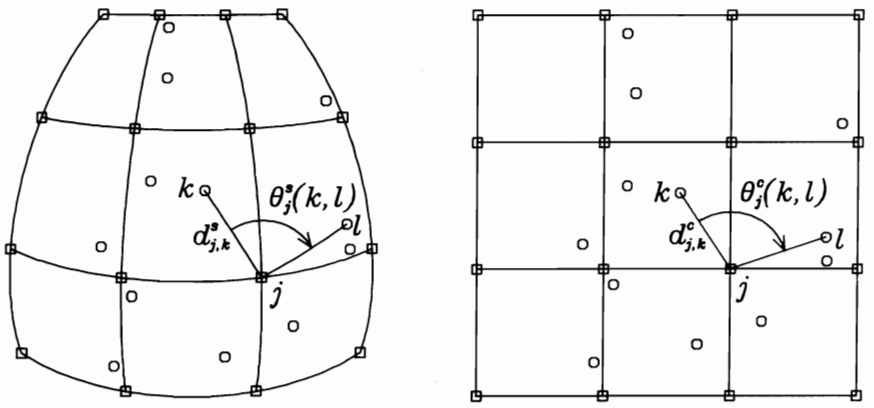


**Figure 1.** Schematic representations of an irregularly distributed set of data points (○'s) and of grid nodes (□'s) a) on the sphere and b) projected into Cartesian two-space. Also illustrated are the corresponding distance ($d^s_{j,k}$ and $d^c_{j,k}$) and directional ($\theta^s_j(k,l)$ and $\theta^c_j(k,l)$) relationships between the data and grid points in spherical (superscript $s$) and Cartesian (superscript $c$) space. It should be noted that $\theta^s_j(k,l) \neq \theta^c_j(k,l)$ or $d^s_{j,k} \neq d^c_{j,k}$, or both.

enth-nearest data point. Four or 10 data points will then lie within the circle (area) of influence represented by the adjusted search radius. Each grid-point value thus represents a constant area of influence—except when fewer than 4 or more than 10 data points fall within the initial search radius—and from 4 to 10 data values.

Thus for each grid point, two sets of $n_j$ ($4 \leq n_j \leq 10$) nearby data points are selected, one set on the basis of Cartesian distances from $j$ in the projected two-space and the other on the basis of distances from $j$ on the surface of the sphere. On the sphere (Figure 1A), $d^s_{j,k}$, the great-circle distance between points $j$ and $k$, is obtained from

$$\cos d^s_{j,k} = \sin \phi_j \sin \phi_k + \cos \phi_j \cos \phi_k \cos (\lambda_j - \lambda_k), \quad (2)$$

whereas Cartesian distance (Figure 1B) is computed from the well-known rectangular-distance formula

$$d^c_{j,k} = [(x_k - x_j)^2 + (y_k - y_j)^2].^{0.5} \quad (3)$$

Superscripts $c$ and $s$, respectively, distinguish Cartesian from spherically-derived distances and angles. When a distance or angle appears without a superscript, it represents either system of geometry. Each set of $n_j$ nearest neighbors then is sorted in ascending order, which results in $d_{j,1}$ and $d_{j,n_j}$ being associated with the nearby data points of minimum and maximum distance from $j$, respectively.

Once ($S_k$, $k = 1,n_j$) have been computed, as in equation (1), Shepard's function corrects for the "directional isolation" of each data point relative to all other nearby data points. Although a few authors (Morrison 1974) have suggested that such adjustments may be inconsequential or even deleterious to accurate reproduction of a known functionally-derived surface, this correction makes theoretical sense (Shepard 1984). Directional isolation of each nearby data point with regard to $j$ is computed from

$$T_k = \sum_{l=1}^{n_j} S_l [1 - \cos \theta_j(k,l)], \quad l \neq k, \quad (4)$$

where $\theta_j(k,l)$ is the angular separation of nearby data points $k$ and $l$ when the vertex of the angle is defined as grid-point $j$ (Figure 1). The angular solitude of a

data point with respect to $j$—on the sphere—is derived from

$$\cos\theta_j^s(k,l) = \frac{\cos d_{k,l}^s - \cos d_{j,k}^s \cos d_{j,l}^s}{\sin d_{j,k}^s \sin d_{j,l}^s}, \quad l \neq k. \tag{5}$$

For points projected into Cartesian space, the separation is obtained from the definition of the angle between two vectors:

$$\cos\theta_j^c(k,l) = \frac{(x_k - x_j)(x_l - x_j) + (y_k - y_j)(y_l - y_j)}{d_{j,k}^c\, d_{j,l}^c}, \quad l \neq k. \tag{6}$$

Thus, data points having a small angular separation contribute less, individually, than points having a large angular separation. With the directional isolation of data-point $k$ known, a combined set of weights is calculated from

$$W_k = S_k^2\left(1 + T_k / \sum_{l=1}^{n_j} S_l\right), \quad l \neq k, \tag{7}$$

which limits the maximum influence of the directional isolation of $k$ to twice the weight based on distance (Shepard 1984); that is, when

$$T_k = \sum_{l=1}^{n_j} S_l. \tag{8}$$

To obtain non-zero gradients on the interpolated surface at data points, increments ($\Delta z_k$) are computed and added to the respective data-point values ($z_k$). The correction involves finding an average weighted gradient for each of the $n_j$ data points within $r_j$ of $j$, based upon the collective rates of change at the other data points within $r_j$. On the surface of the sphere, the incremental corrections are obtained for each of the data points associated with $j$ from

$$\Delta z_k = \left\{\left[\frac{\overline{\partial(\Delta z)}}{\partial\lambda}\right]_k d_\lambda^s(j,k) + \left[\frac{\overline{\partial(\Delta z)}}{\partial\phi}\right]_k d_\phi^s(j,k)\right\} \times \{v/(v + d_{j,k}^s)\}, \tag{9}$$

where $\overline{\partial(\Delta z)}/\partial\lambda$ is the average partial derivative with respect to longitude, $\overline{\partial(\Delta z)}/\partial\phi$ is the average partial derivative with respect to latitude, $d_\lambda^s(j,k) = (\lambda_j - \lambda_k)\cos\phi_j$, and $d_\phi^s(j,k) = \phi_j - \phi_k$. The average partial derivatives are taken as

$$\left[\frac{\overline{\partial(\Delta z)}}{\partial\lambda}\right]_k = \frac{\sum_{l=1}^{n_j} W_l(z_l - z_k) d_\lambda^s(l,k) d_{k,l}^{s\,-2}}{\sum_{l=1}^{n_j} W_l}, \quad l \neq k, \tag{10}$$

and

$$\left[\frac{\overline{\partial(\Delta z)}}{\partial\phi}\right]_k = \frac{\sum_{l=1}^{n_j} W_l(z_l - z_k) d_\phi^s(l,k) d_{k,l}^{s\,-2}}{\sum_{l=1}^{n_j} W_l}, \quad l \neq k, \tag{11}$$

where $d_\lambda^s(l,k) = (\lambda_l - \lambda_k)\cos\phi_k$ and $d_\phi^s(l,k) = \phi_l - \phi_k$, whereas a somewhat arbitrary adjustment is made to limit the influence of the increments to one-tenth the data range, so $|\Delta z_k|$ cannot exceed $0.1(\max z_i - \min z_i)$, where $i$ again refers to any data point on the map. Although not obvious, the limit of $|\Delta z_k|$ can be deduced from equation (9) and the Cauchy-Schwarz inequality. The adjustment parameter ($v$) takes the form

$$v = \frac{0.1(\max z_i - \min z_i)}{\max\left[\left(\left[\frac{\overline{\partial(\Delta z)}}{\partial\lambda}\right]_k\right)^2 + \left(\left[\frac{\overline{\partial(\Delta z)}}{\partial\phi}\right]_k\right)^2\right]^{0.5}} \tag{12}$$

Forms of (9) through (12) are also used for Cartesian-based computations with $\overline{\partial\Delta z}/\partial x$, $d_x^c(j,k)$, $\overline{\partial\Delta z}/\partial y$, $d_y^c(j,k)$, $d_{j,k}^c$, $d_x^c(l,k)$, $d_y^c(l,k)$, and $d_{k,l}^c$ replacing $\partial\Delta z/\partial\lambda$, $d_\lambda^s(j,k)$, $\partial\Delta z/\partial\phi$, $d_\phi^s(j,k)$, $d_{j,k}^s$, $d_\lambda^s(l,k)$, $d_\phi^s(l,k)$, and $d_{k,l}^s$, respectively.

With evaluation of these functions, the value predicted at grid point $j$ ($\hat{z}_j$) becomes

$$\hat{z}_j = \begin{cases} \sum_{k=1}^{n_j} W_k(z_k + \Delta z_k) / \sum_{k=1}^{n_j} W_k, & d_{j,1} > \epsilon \\ m^{-1} \sum_{k=1}^{m} z_k, & d_{j,1} \leq \epsilon, \end{cases} \tag{13}$$

where $m$ is the number of data points within $\epsilon$ of grid point $j$. Thus, when one or more data points are sufficiently close to a grid point (that is, within $\epsilon$ of $j$), the grid point takes on their average value;

otherwise, part one of equation (13) defines the interpolation function. On the surface of the sphere, $\epsilon$ is specified as the maximum of a function of grid-cell longitudinal difference ($\Delta\lambda$) and latitudinal range of the grid points; or grid-cell latitudinal difference ($\Delta\phi$):

$$\epsilon^s = \begin{cases} 0.01\max\{0.5\Delta\lambda[\cos(\max\phi_j) + \cos(\min\phi_j)],\Delta\phi\}, \\ \quad (\max\phi_j)(\min\phi_j) \geq 0.0 \\ 0.01\max\{0.5\Delta\lambda[\cos(\max|\phi_j|) + 1],\Delta\phi\}, \\ \quad (\max\phi_j)(\min\phi_j) < 0.0, \end{cases} \quad (14)$$

where $\max\phi_j$ and $\min\phi_j$ are the largest and smallest latitudes, respectively, found among all the grid points, and $\max|\phi_j|$ is the grid latitude of greatest magnitude. In other words, when the grid points lie entirely within either the northern or southern hemisphere, $\epsilon^s$ is computed from part one of equation (14), whereas part two of equation (14) is evaluated if the grid spans the equator. For points in Cartesian two-space,

$$\epsilon^c = 0.01\max(\Delta x,\Delta y), \quad (15)$$

where $\Delta x$ is the width and $\Delta y$ is the height of a typical rectangular grid cell. With these modified versions of Shepard's algorithm, point interpolations from irregularly spaced data points can be performed for any bounded rectangular or spherical lattice, as well as for any spherical grid that spans the surface of the globe.

## Isoline Construction

Once data values have been estimated at all nodes of a lattice, the gridded data field must be described by the fitting and subsequent plotting of isolines. Cartesian-based methods of contour-lacing are well known (McCullagh 1981), but we needed a spherically based lacing routine to position the isolines on the surface of the sphere in order not to contaminate the presentation of a spherically interpolated field with a projection-related lacing error.

Our primary lacing unit is either a spherical ($\Delta\lambda$-by-$\Delta\phi$) or a Cartesian ($\Delta x$-by-$\Delta y$) grid cell whose vertices are defined by 4 grid points (Figure 2). Each grid cell is quartered by the definition of a grid-cell "center" and the construction of "half-diagonals" extending from each

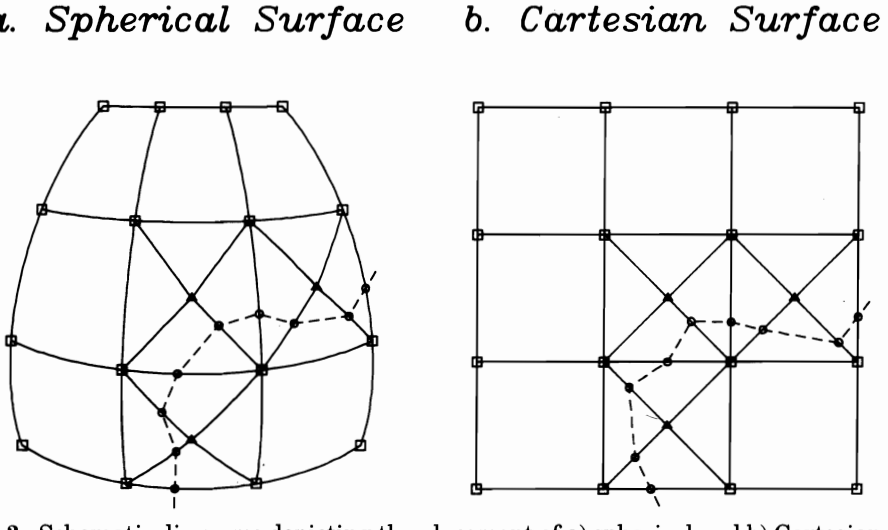


**Figure 2.** Schematic diagrams depicting the placement of a) spherical and b) Cartesian grid-cell centers (△'s) and the subdivision of each grid cell into four triangular sub-cells. A hypothetical isoline (dashed) has been laced through the triangular mesh—intersecting the edges of triangular sub-cells at points (○'s) determined by either great-circle or linear interpolation between the end-point values of the intersected edges—to illustrate the contour-placement procedure.

of the grid-cell corners to the center. On the sphere, the center is located at the average latitude and longitude of the cell, and the half-diagonals are arcs of great circles. In Cartesian two-space, however, the center and half-diagonals are defined by the intersection of diagonals of a grid quadrilateral (cell), which has as its vertices 4 projected grid points. Within each spherical or Cartesian grid cell, four triangles are thus created. At the vertex shared by the four triangles (the cell center), a value is estimated as the arithmetic mean of the four corner values, although this computation can be a source of error. When the cell size is relatively small, as with the maps next discussed, the error is insignificant. On the other hand, when the lattice is coarse, the center point and its associated value should be more accurately determined. With the definition of a triangular mesh and estimation of center-point values, all desired isolines can be unambiguously positioned within the interpolated scalar field.

From an initial point on or intersection with the edge of a first triangle, an isoline must pass through the triangle and intersect one of two opposite sides at a point determined by the relative magnitudes of the values associated with the end points of the intersected edge. The coordinates of each intersection are recorded. As the second intersection positions the isoline on an edge of a triangle adjacent to the first, the process may be repeated for the second triangle and the coordinates of a third intersection stored. Then a third triangle adjacent to the second may be evaluated and so on until the isoline either crosses a map boundary or closes itself. By successively reproducing these calculations for the desired number of contour levels, a complete isoline representation of the gridded data field can be computed and stored.

From the series of intersection coordinates associated with the desired isolines, Cartesian-derived contour lines have merely to be scaled and plotted—along with such supportive information as a similarly projected graticule or land-area outline—to produce a map. Coordinate points associated with isolines constructed on the sphere, as well as any background information, must be projected prior to scaling and plotting.

## A Comparison of Spherically and Cartesian-derived Annual Air-Temperature Maps

To illustrate the degree and nature of error which can be produced on small-scale climate maps by projection of data points prior to interpolation to a regular grid and contouring, we sampled and alternately mapped annual average air temperature (°C) in the northern hemisphere with both spherically and Cartesian-based interpolation and contouring procedures. Using the data set compiled by Willmott, Mather, and Rowe (1981), we randomly drew 100 stations from the subset of stations bounded by $-170° \leq \lambda \leq -50°$ and $2° \leq \phi \leq 90°$, which resulted in a markedly uneven distribution of station locations (Figures 3 and 4). We used two cylindrical map projections, Lambert's equal-area and Miller's, to examine projection-related dissimilarities that can occur between isotherms estimated on the spherical surface prior to projection and isotherms determined in Cartesian two-space from a previously projected set of data points. We examined cylindrical projections because they comprise the largest group of projections used to portray meso- and macro-scale climate fields. An experimental version of MAPRO performed projection-related translations (Kansas Geological Survey 1981); the land-area outlines were taken from WORLDDATABANK I (Central Intelligence Agency 1972).

Our interpolation began by superimposing a lattice 4° of latitude by 5° of longitude—a grid size frequently used in global climate models—over the area to be mapped. Using spherical distance and directional relationships between the data and grid points, we initially computed grid-point estimates of air temperature and, subsequently, iso-

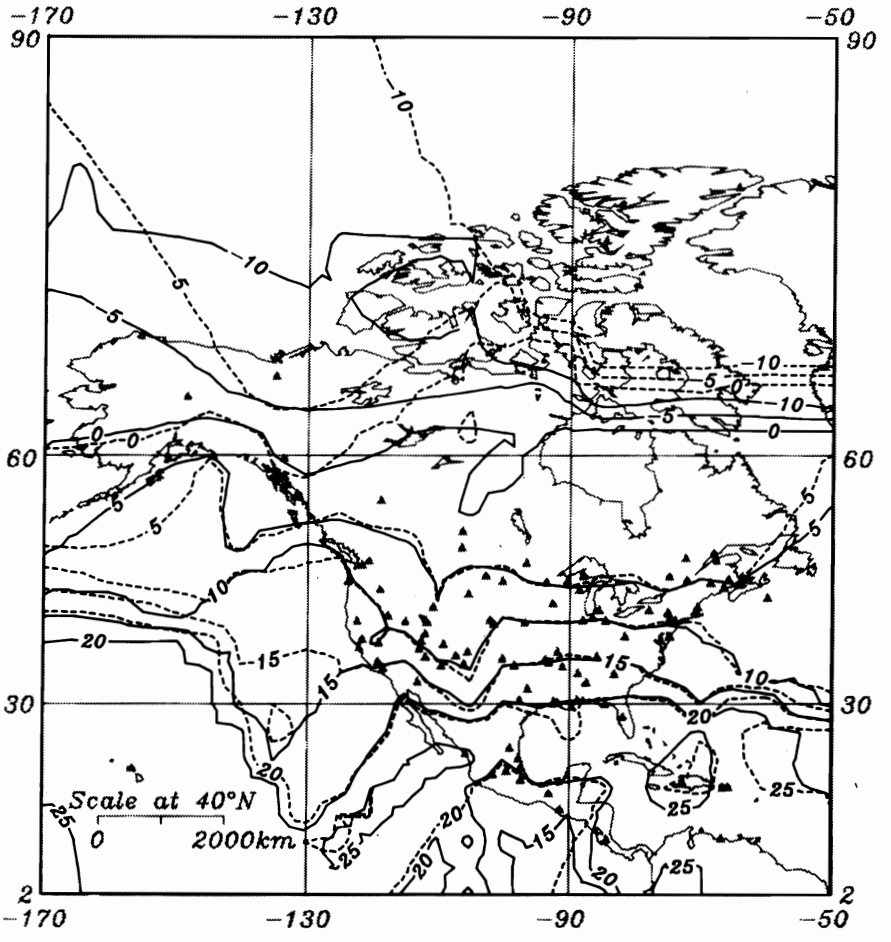


**Figure 3.** Isothermal representations of mean annual shelter-height air temperature (°C) over the western half of the northern hemisphere using Miller's cylindrical projection. From 100 irregularly-spaced data points (△'s), temperatures were interpolated to a regular 4°-by-5° lattice and subsequently contoured. The solid isotherms represent interpolation and contouring on the surface of the sphere *prior to* Miller's projection, whereas the dashed isotherms depict interpolation and contouring in Cartesian two-space *following* Miller's projection of the data points into two-space.

therm positions. The λ and ϕ coordinates associated with each spherically estimated isotherm and map were then twice projected into Cartesian two-space (with Lambert's equal-area and Miller's projections). We next constructed two comparable Cartesian-derived isotherm maps by producing two projected sets of data points—again using Lambert's and Miller's projections—from each of which we made Cartesian-based interpolations to a correspondingly projected (now rectangular) 4°-by-5° grid. The two Cartesian-estimated, grid-point air-temperature fields were each separately contoured within their respective projected Cartesian spaces.

Before examining individual differences between spherically and Cartesian-derived isotherm patterns, we should mention certain characteristics that the maps presented here have in common, largely owing to assumptions embodied in Shepard's algorithm (Figures 3 and 4). Where the station network is sparse, both the spherical and

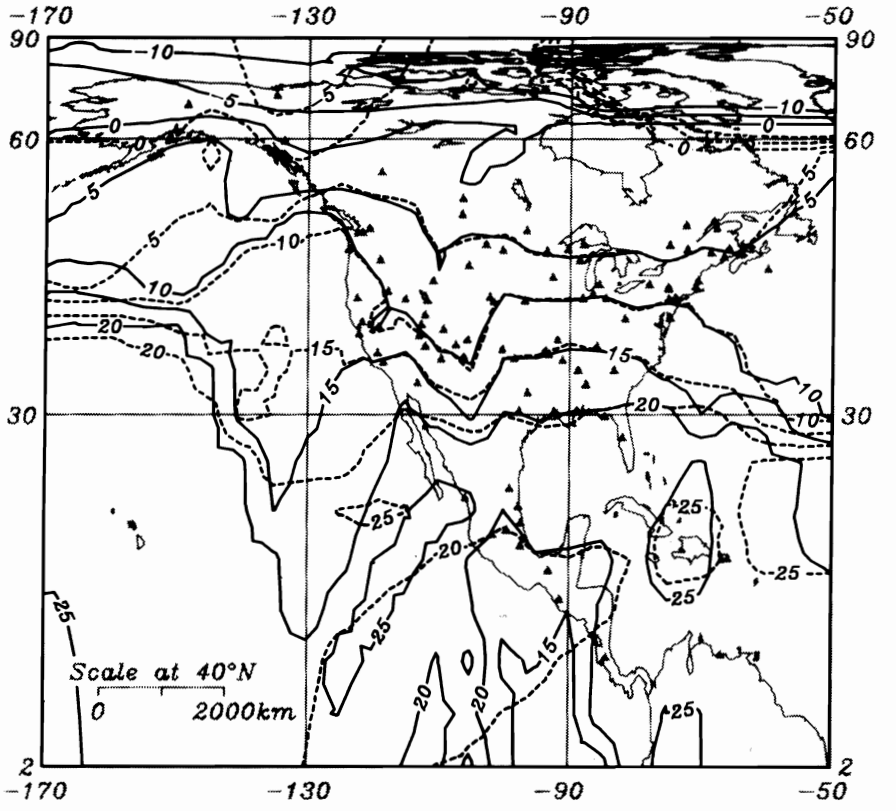


**Figure 4.** Isothermal representations of mean annual shelter-height air temperature (°C) over the western half of the northern hemisphere using Lambert's cylindrical equal-area projection. From 100 irregularly-spaced data points (△'s), temperatures were interpolated to a regular 4°-by-5° lattice and subsequently contoured. The solid isotherms represent interpolation and contouring on the surface of the sphere *prior to* Lambert's projection, whereas the dashed isotherms depict interpolation and contouring in Cartesian two-space *following* Lambert's projection of the data points into two-space.

Cartesian versions of Shepard's function will extrapolate into the voids in such a way that the gradient of the temperature surface will diminish with distance from the nearest data points, explaining why, for instance, the isotherms spread apart between Hawaii and Central America. In a few instances, where a large area contains but a single observation, the data point over-influences nearby and not-so-nearby grid points, flattening the interpolated surface around the data point, for instance, around Hawaii. Consequently, near the edge of the flattening the surface gradient must increase rapidly to accommodate the influence of "new" data points that have come within the search radii of the local grid points. The steep north-south gradient between Hawaii and Alaska at approximately 40°N latitude, shown by the convergence of the isotherms (Figures 3 and 4), exemplifies this errant tendency.

To avoid an extra computational expense, we did not attempt to smooth the isotherms; therefore, they have a slightly jagged appearance. At the scale these maps are presented, however, the lattice is relatively fine, so the maps' appearance is not seriously compromised. This relatively fine grid texture allows a certain clarity of interpretation since the error exhibited by the Cartesian-derived

isolines is ascribable to the interpolation process even though, generally speaking, isoline misplacements are compounded by contouring errors.

When the relationships between data and grid points on the sphere are preserved during contouring, relative isotherm positions remain constant regardless of the map projection (Figures 3 and 4). Yet where data points are projected prior to Cartesian-based interpolation and contouring, isotherm locations relative to each other and to supplemental map information (land-area outlines and data-station locations) will inconsistently change from one irregularly spaced station distribution to another, as well as from one projection to another. The inconsistency with which such errors appear, from data set to data set, and from projection to projection, results from synergism among data-point distribution, lattice pattern, and error inherent in the map projection selected. The error field on such a map may well be a unique result of the combined influences of these three factors and, therefore, difficult to evaluate. When isotherms also are estimated on the sphere, however, they can be compared to the Cartesian-derived isotherms for any particular map of interest.

Miller's cylindrical projection—in combination with the data- and grid-point distributions—produced the most striking differences between spherically and Cartesian-estimated isotherm locations (Figure 3). In the high latitudes, where the projection is highly exaggerated and data points are few, there is marked disparity between the two sets of isotherm patterns. When corresponding spherically and Cartesian-interpolated grid-point values were subtracted from each other, the magnitudes of the differences in the higher latitudes ($\phi > 60°$) frequently exceeded 5° or 10°C. The Cartesian-derived isotherms generally fall north of their spherically computed counterparts because the projection places data points progressively further apart as the pole is approached. Another expression of the high-latitude error field is the Cartesian-derived −5° and −10°C isotherms that head northwest from about 70° north latitude, the cooler of the two ultimately passing through the pole. Annual isotherms ring the poles—as is evident among the spherically-derived isotherms—so there is only a slim possibility that the Cartesian-derived −5° and −10°C isotherms are correct. Such errors are common when Cartesian-based interpolations are made within cylindrically projected two-space, though in this instance the errant tendency is intensified by Shepard's constraint on the extrapolated surface gradient. Where the data points are most dense, as in the United States, agreement between the two isotherm systems is best, although discrepancies still exist.

On Lambert's cylindrical projection, where latitude is compressed near the pole to maintain equivalence, error magnitudes resemble those of Miller's projection (Figure 4). In this instance, however, the data points are placed nearer each other as they approach the pole, creating an unrealistically high local variance in air temperature at the higher latitudes. Since the Cartesian-based interpolation and contouring procedure treats the pole as a line on cylindrical projections, the abnormally high variance in temperature creates large fluctuations in the interpolated field and its isothermal representation. Often this erroneously causes multiple isotherms to pass through the pole. Again, within the area where the distribution of data points is most dense, the spherically and Cartesian-derived isotherms agree, but not perfectly.

Such symptoms are typical of Cartesian-based cylindrically-projected maps, especially when the map surfaces include high latitudes. Also, when a cylindrically projected map encompasses the full, 360° range of longitude, east-west trending isolines typically fail to connect at the common longitude represented by the map's vertical edges. Such errors exist on *all* small-scale Cartesian-derived isoline maps, although their identification is often difficult because a

map may not extend to at least one of the poles or over 360° of longitude; the interpolation or contouring process may be constrained near map borders to make the map appear correct; or too little information about interpolation and contouring methods is provided for the map reader to make a meaningful evaluation. For these reasons, we recommend that interpolation to a regular lattice and contouring should take place on the surface of the sphere, followed by projection of isolines and other map information.

## SUMMARY AND CONCLUSION

We have presented a sensitivity study of the errors which can result on small-scale climate maps from the common practice of projecting data points prior to interpolation and contouring. Working from Shepard's (1968 and 1984) well-known local-search interpolation function, we have developed and described two algorithms that perform the interpolation and contouring process both on the surface of the sphere and in Cartesian two-space. To illustrate the nature and magnitude of differences that can occur between spherically and Cartesian-derived interpolations and contours, we mapped mean annual air temperature over the western half of the northern hemisphere, represented by 100 randomly selected stations, with both algorithms on two well-known cylindrical map projections: Lambert's equal-area and Miller's.

When we superimposed spherically derived isotherm maps—assumed to be correct—over Cartesian-interpolated and contoured maps, the error fields generated by the Cartesian approach became apparent. Local errors as large as 5° to 10°C commonly appeared in those regions containing few data stations or with large projection distortion. However, when a Cartesian-derived, small-scale climate map encompasses most of the globe, two characteristic errors can often be discerned without reference to a spherically-derived standard: frequently, more than one isoline passes through a pole or east-west trending isolines do not meet at the common longitude represented by the vertical edges of the map.

Our findings strongly suggest that the interpolation to grid points and subsequent contour lacing on small-scale climate maps should, in virtually all cases, be carried out on the surface of the sphere. Otherwise, calculations performed on the interpolated grid-point values or climatic inferences made from the isoline representations of raw and gridded data fields will be in error. Since our spherically and Cartesian-based versions of Shepard's algorithm and their accompanying contour-lacing procedures are logically identical—except that one set computes spherical distances and directions, and the other Cartesian—our findings further suggest that comparable errors will result from the use of *any* Cartesian-based interpolation and contouring method.

## REFERENCES


Akima, H. 1978. A method of bivariate interpolation and smooth surface fitting for irregularly distributed data points. *ACM Transactions on Mathematical Software* 4, no. 2:148–59.

Barnes, S. L. 1964. A technique for maximizing details in numerical weather map analysis. *Journal of Applied Meteorology* 3:396–409.

Central Intelligence Agency. 1972. *WORLDDATABANK I.*

Cressman, G. P. 1959. An operational objective analysis system. *Monthly Weather Review* 87:367–74.

Fritsch, J. M. 1971. Objective analysis of a two-dimensional data field by the cubic spline technique. *Monthly Weather Review* 99:379–86.

Gandin, L. S. 1963. *Objective analysis of meteorological fields.* Leningrad: Gidrometeorologicheskoe Izdatel'stvo. (Translated from Russian by the Israel Program for Scientific Translation, Jerusalem, 1965, 242 pp.)

Halem, M., Kalnay, E., Baker, W. E., and Atlas, R. 1982. An assessment of the FGGE satellite observing system during SOP-1. *Bulletin of the American Meteorological Society* 63:407–26.

Kansas Geological Survey. 1981. *MAPRO* (personal communication).

Marble, D. F., ed. 1981. *Computer software for spatial data handling.* Ottawa: International Geographical Union, Commission on Geographical Data Sensing and Processing.

McCullagh, M. J. 1981. Creation of smooth contours over irregularly distributed data using local surface patches. *Geographical Analysis* 13:51–63.

Morrison, J. L. 1974. Observed statistical trends in various interpolation algorithms useful for first stage interpolation. *The Canadian Cartographer* 11:142–59.

Panofsky, H. A. 1949. Objective weather-map analysis. *Journal of Meteorology* 6:386–92.

Peucker, T. K. 1980. The impact of different mathematical approaches to contouring. *Cartographia* 17, no. 2:73–95.

Rhind, D. 1975. A skeletal overview of spatial interpolation techniques. *Computer Applications* 2:293–309.

Rivin, G. S., and Kulikov, A. I. 1982. Mapping fields of the meteorological elements given at the nodes of a latitude-longitude grid. *Meteorologiya i Gidrologiya* 1:41–48 (page range on the translation: pp. 31–37).

Sampson, R. J. 1978. *SURFACE II graphics system (revision one)*. Lawrence, Kansas: Kansas Geological Survey.

Schlatter, T. W., Branstator, G. W., and Thiel, L. G. 1976. Testing a global multivariate statistical objective analysis scheme with observed data. *Monthly Weather Review* 104:765–83.

Shepard, D. 1968. A two-dimensional interpolation function for irregularly-spaced data. *Proceedings—1968 ACM National Conference,* pp. 517–24.

———. 1984. Computer mapping: The SYMAP interpolation algorithm. In *Spatial statistics and models,* eds. G. L. Gaile and C. J. Willmott, pp. 133–45. Dordrecht, Holland: D. Reidel.

Wahba, G. 1979. *Spline interpolation and smoothing on the sphere.* Department of Statistics Technical Report no. 584, University of Wisconsin, Madison,

———. 1981. Spline interpolation and smoothing on the sphere. *SIAM Journal of Scientific and Statistical Computing* 2, no. 1:5–16.

Wahba, G., and Wendelberger, J. 1980. Some new mathematical methods for variational objective analysis using splines and cross validation. *Monthly Weather Review* 108:1,122–43.

Willmott, C. J., Mather, J. R., and Rowe, C. M. 1981. Average monthly and annual surface air temperature and precipitation data for the world: Part 2. The western hemisphere. *Publications in Climatology* 34, no. 2.